# Geology and Fluid Inclusions Studies of Molybdenite Mineralization in Granites of Gabal Gattar, North E Astern Desert, Egypt

Essam M. Esmail

Nuclear Materials Authority, Cairo, Egypt
essam_12mem@yahoo.com

**Abstract:** In Gabal Gattar, Mo and U mineralization are located near the northern margin of the granitic mass of Gabal Gattar, they are hosted in the high silica granites. They were concentrated at the late stage of granite palotonism in a volatile rich fractionate which was deposited by a shallow hydrothermal system a long structures in granite mass. The U mineralization concentrated in deformed and hydrothermal granite and controlled by NNE – SSW to NW – SE structures, while the Mo mineralization is hosted in quartz veins striking NS. Fluid inclusion studies can contribute in the understanding of physico-chemical conditions controlling the genesis of molybdenite mineralization, and to suggest the fluid evolution model of these mineralizations. Both quartz veins and their hosted uraniferous granites in the Gabal Gattar area are choicen in the present study. Taking all available information into consideration, the following model of fluid evolution is suggested. There are two stages of mineralizing fluids. The oldest recorded fluid is represented by remnants that are only preserved in granitic samples as a result of strong acidic hydrothermal fluids where oxidation of molybdenite to ferro-molybdenite (Fe2(Mo4)3.H2O) in granite is significance. These fluids are rich of water of pure NaCl system, low saline (1.73 to 11.70 wt% NaCl eq.) and with homogenization temperature (Th°C) values around 200°C. The tectonic history of the region and oxidation patterns confirm the fluid inclusion data that oxidation may have begun at high pressure 19.7 k.bar and reach to about 5.7 k.bar However the pH can remain above the stability field of Mo when alkaline hydrothermal solution are affected the granites and alternatively it will be free to migrate and supergene enrichment of Mo in the form of molybdenite, will apply where there are only minor amounts of pyrite and increasing in $H_2S$ fugacity then precipitate along the week fractured quartz vein surfaces. The detailed fluid inclusions study in the molybdenite bearing-quartz veins is in harmony with the previous modeling where it indicates that the last fluids are homogenized at lower temperature (ranging from 126.7 to 170°C) due to cooling with addition of some divalent salts ($MgCl_2 \pm CaCl_2$) as a result of wall-rock interaction. These fluids are generated under lower pressure (from 4 to 5 k. bar) and characterized with high salinity (14.7 to 23.3 wt% NaCl eq**.).** Finally it can be concluded that subsequent cooling and change in the pH are considered the two factors that have triggered molybdenite precipitation.

**[**Essam M. Esmail**. Geology and Fluid Inclusions Studies of Molybdenite Mineralization in Granites of Gabal Gattar, North E Astern Desert, Egypt.** *Nat Sci* 2018;16(2):124-133]. ISSN 1545-0740 (print); ISSN 2375-7167 (online). http://www.sciencepub.net/nature. 18. doi:10.7537/marsnsj160218.18.

**Keywords:** Geology, Fluid Inclusionsm Molybdenite, Mineralization, Granites of Gabal Gattar, North E Astern Desert, Egypt

## Introduction

Molybdenite is a mineral, though seldom seen in rocks, of molybdenum disulfide, $MoS_2$ and is the primary source of molybdenum. It is environment disseminated as flakes and tiny crystals in igneous rocks and infrequently in larger crystals in simple pegmatites. Molybdenite occurs as an exsolution mineral in the later stages of crystallisation of granitic magma occupying interstitially between silicate minerals, fracturs and cavities. Bjorn (1985)**,** suggested that the granites associated with molybdenite occurrences were probably generated by partial melting of earlier igneous rocks, or they may be of sub-crustal origin, the large granite bodies originated by partial melting of Archean continental crust. According to isotopic data, Ixer and Odling (1985) concluded that the source of the molybdenite mineralization and the granite magma was probably the Pan-African continental crust with contributions from the mantle. Carten et al (1988 a and b) recorded all the higher temperature assemblages molybdenite mineralizations, which can be treated in terms of two simplified mineral assemblages that are related to veins filled with quartz + fluorite ± molybdenite. Seedorff and Einaudi (2006) study the low homogenization temperature Mo-mineralizations ($T_h$°C) is ranging from 530 to 210°C) in Colorado, which include all the previous higher temperature assemblages.

Molybdenite deposits in Egypt are recorded in four main localities in the northern part of the Eastern Desert. These localities are Gabal Gattar, Gabal Abu Marwa, Gabal Abu Harba and Gabal Umm Disi, Gabal Gattar molybdenite deposits are considered to

be the largest. (Dardier et al., 1983 and Said, 1990). The dissemination of the molybdenite in the country rock, on both sides of the quartz veins and its presence at the contact with the granitic country rock may indicate the mineralizing solutions shortly followed the intrusion of quartz veins (Dardier et al, 1983). The presence of muscovite, cavities feldspar crystals as well as developed molybdenite crystals may indicate the mineralized solutions were limited and subsequent to the granitic intrusions (Dardier et al, 1983). Helmy (1999) studied the mineralogy, fluid inclusion, geochemistry of Mo-U fluorite in Gabel Gattar and concluded that both Mo and U-F mineralization were evolved from the same granitic magma. Salem, et.al (2003) studied the geological and fluid inclusion constraints of the genesis of hydrothermal U deposits, Northeastern Desert, Egypt. They are concluded that the epithermal origin for uranium mineralization at Gattar area.

The present study deals with the more low temperature molybdenite mineralization. A reconnaissance fluid inclusions study was conducted primarily to determine the fluid characteristics of each molybenite mineralization in both quartz vein and hosted uraniferous granite based on microthermomertic measurements for incorporation into a model of the geochemical evolution of the hydrothermal system.

**Geological sitting**

The area is essentially composed of pink to red granites of Gabal Gattar. It is located at the northwest of Hurghada city. The study area is enclosed between longitudes 33° 14′ and 33° 20′ E and latitudes 27° 04′ and 27° 08′ N (Fig.1a). Gabal Gattar younger granites have been affected by several post magmatic hydrothermal fluids caused the different type of alterations; includes hematitization, kaolintization, fluoritizaton, and epidotization besides silica introduction along uranium and molybdenium mineralization into fractures (Salman et al., 1999). Later alteration processes were superimposed on such alteration zones such as episyentization, carbonatization and bleaching (El Kalioby et al., 2003 and Shalaby et al., 2009). Gabal Gattar granite acquired its importance from hosting uranium mineralization in many occurrences (Fig. 1a). Generally, the anomalous radioactivity is essentially associated with strongly hematitized and silicified-kaolinized sheared granitic zones, mainly along major NNE-SSW and NW-SE faults (Mahdy, 2011). The area of Gabal Gattar was affected by various tectonic episodes accompanied with different types of hydrothermal solutions having various compositions, which caused the different alteration types. The alterations of the granite are classified into the following three main types, in a decreasing order of abundance:- (1) ferrugination, (2) kaolinization and (3) silicification. El-Zalaky (2002), Salman et. al., (2005) and Abd El Hamid (2006) suggested that the emplacement of Gattar pluton has led to the formation of weak zones, fractures and faults around the peripheral parts, which facilitate the action of the hydrothermal solution that carrying uranium mineralization. Esmail (2005) and Amin (2010) considered the shear zones and fault planes, as well as contacts provided the channel-ways for the circulating hydroihermal solutions. The Gabal Gattar area has been subjected to different tectonic phases. The structural elements of the area can be considered representing two stages of deformation namely: ductile and brittle deformations. These deformational episodes produce different styles and variable trends of joints, faults, shear zones and other fractures.

Joints are projected and contoured graphically presented by a contour diagram (Fig.1b); four main trends have been recognized. The first predominant set strikes NNE-SSW and is very steeply, mainly dipping to ESE and WNW with an angle of about $80^{o}$. The second abundant set is directed NE- SW and is dipping $80^{o}$ to NW, while the joints dipping to the SE have an angle of $70^{o}$, the third joint set directing to the N-S have an average angle of $70^{o}$ and dipping mainly to W. The fourth common sets are trending to the WNW-ESE.

Gabal Gattar pluton is actually dissected by several fractures and faults, which trend mainly in NNE-SSW, NNW-SSE, NW-SE and N-S directions (Fig.1c). They are only invaded by basic and rarely intermediate dykes. Some aplite and pegmatite dykes and pockets are encountered.

The geological study of Gattar area doesn't report the presence of field relationship between uranium, and molybdenite mineralization. The molybdenite deposits of Gabal Gattar lies in the northern part of Gabal Gattar granite massif, at a distance of 65 km from the Red Sea coast north of Hurghada by 15 km. Mahdy et. al, (2015) studied that Gattar batholith is divided into two distinctive areas, the southern part (Syenogranite), while the northern part (alkali feldspar granite). The two different granitic rocks are magmatic in origin and have A-type characteristics generated by partial melting. U and Mo mineralization is limited to the margin of the highly evolved alkali feldspar granites.

Ghobrial and Lotfi (1967) stated that during the deutric phase, Mo was leached from some places especially the tectonized ones with fractures and redeposit in the silica vein as an economic Mo deposits. The molybdenite mineralizations of Gabal Gattar area are represented mainly by quartz veins and its hosting bearing granite. The quartz veins bearing molybdenite are typically coarse free from mafic

minerals and found that chalcopyrite and pyrite were existing in the molybdenite deposits, indicating that this deposit have hydrothermal origin (Schurmann, 1966).

Molybdenites are found in two forms; (1) as crystals that are irregularly distributed in quartz veins and veinlets. They are well developed showing length variation between 2 and 3 cm. (2) as massive ore at wall rock confined to areas between molybdenite crystals bearing quartz veins and the grantic host rocks. The ore zone occupies the topmost hills of Gabal Gattar granites. It is present in the form disseminated fine crystals or a group of thin quartz veinlets crossing the most rugged and inaccessible part of the area. Their thickness ranges from 10 mm to 20 mm only.

Dardier et al. (1983), indicated that four types of the molybdenite ore deposits in Gabal Gattar granites. The first one is the coarse crystalline deposits which predominate in the quartz veinelts within the granitic country rocks. The second type is the wall rocks in which represent a thin film of molybdenite between the ore bearing quartz vein and the granitic country rocks. The third one is the thin quartz veinlets type while the fourth type is that disseminated as the molybdenite crystals in the granitic host rocks.

**Petrography of Mo Bearing Quartz Vein and Granites**

The study of polished section of these samples revealed that molybdenite occurs mainly as euhedral crystals with its characteristic two sets of cleavage and polysynthetic twinning (Fig.2a). It is also found as the tabular or needle crystals filling the fracture of the gangue minerals (Fig.2b). The sulphide minerals are represented by pyrite and which is disseminated in the quartz veins (Fig.2c). The texture exhibited by this mineral always according the gangue minerals and filling the fractures of the rock implies its crystallization as a late hydrothermal phase (Fig.2d and e).

The ferro-molybdenite crystals occur as medium to coarse grained plates, sometimes curved, having undulatory extinction. The ferro-molybdenite is coated with iron oxide representing an oxidic mineralization (Fig.3a).

A ferro-molybdenite crystal is developed between quartz crystals (Fig.3b and 3e). The opaque minerals are represented by fine grained hematite and goethite. They commonly fill cracks in the gangue or form patches with distinct colliform texture (Fig.3c); they rarely occur as scattered elongated crystals. Minute crystals of K-feldspar coat the molybdenite crystals or are developed separately near them (Fig.3d).

**Distribution of u & th in mo bearing rocks**

Chemical analyses for U (in ppm) were detected using UA3 technique as well as spectrometric method was used for Th determination. U contents are ranging from 0.5 to 3 ppm and from 5 to 6 ppm in quartz vein and hosting granite respectively. In the granitic samples Th contents range from 25 to 29 ppm for granitic samples and from 2 to16 ppm in quartz vein samples. Th/U ratios ranging from 4 to 6 ppm which the same range of mantel derived potassic granites (Rogers and Adams, 1969).

**Fluid inclusion study**

The representative samples from mineralized quartz veins as well as the hosted uraniferous granite were chosen for fluid inclusion studies. Double polished thin sections of the selected samples (250-300 μm) were prepared. The freezing/heating behavior of the fluid inclusions where the temperature at which phase change took place were recorded using a fluid inclusion adapted USGS gas flow heating / freezing stage mounted to petrographic microscope. Heating runs were carried out with heating rates of 6°C / minute until homogenization was considered to be approached. Homogenization temperature ($T_h$°C) was determined as the mean of the highest temperature where a gas bubble was present and the lowest temperature where a gas bubble did not observe. All inclusions in the studied samples homogenized to a liquid phase. Reproduce ability of the measurements is approximately ± 1°C. Thermocouple accuracy was ± 0.1°C over the investigated interval 0 to - 40°C.

Fluid inclusions were then frozen by super cooling to temperature between -70 and -90°C. The frozen inclusion were then heated 1 –2 °C / minute and the melting temperatures of the solid phases formed during freezing were recorded. Low temperature microthermometry was performed on cooling stage using an Olympus optical microscope (objective X80), to measure the eutectic, ice melting temperatures (respectively $T_e$ and $T_m$). According to the calibration curves, ice melting temperatures are given with an error of about ±1°C, whereas the errors on the first melting temperatures may have reached ±5 °C and more for small fluid inclusions (< 5 μm) because of the difficulty observing the exact eutectic melting. The final ice melting temperatures ($T_m$°C) enable collections of fluid inclusion salinities, which are expressed as NaCl wt.% equivalent and was calculated from measurements of the ice melting temperature ($T_m$ ice) using the equations of Bodnar (1993) for aqueous inclusions using Bulk computer program after Baker (2003).

Suitable fluid inclusions were studied in vein-filling minerals and their hosting granite. Characteristics of fluid inclusions were studied under an optical microscope with objective X50, and

standard petrographic observations were recorded. Fluid inclusions are abundant in quartz vein samples. Fluid inclusions occur as single inclusions, cluster and secondary trails. A small number of fluid inclusion are trapped during the growth of surrounding host crystals and occur as isolated groups, sometimes confined within growth zone of quartz crystals and these assumed to be primary. A great number of fluid inclusions are related to fractures, and therefore, these inclusions were assumed to be secondary Fig. (4a and b). Inclusions shapes may vary from negative crystals to subspherical or irregular branched shapes (obviously necked down) and dimensions range from 10 to 30 mm. Primary fluid inclusions in quartz are found in both two-phase, water-rich at room temperature, with constant liquid/ vapor ratio at ~95:5 and one aqueous phase. No microthermometric evidences of $CO_2$ have been found in any fluid inclusions described above. The results presented in table (1) are referred to the primary fluid inclusions.

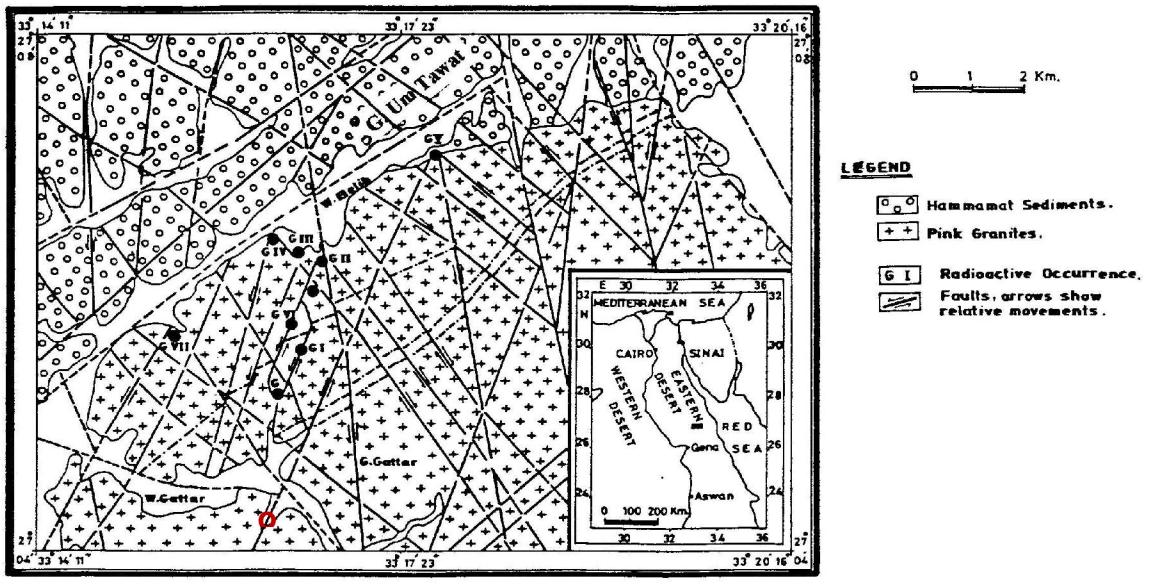


Fig. (1a): Geological – Structural map of the area of Gabal Gattar Sample location { **O** } (after Shalaby and Moharem, 2001)

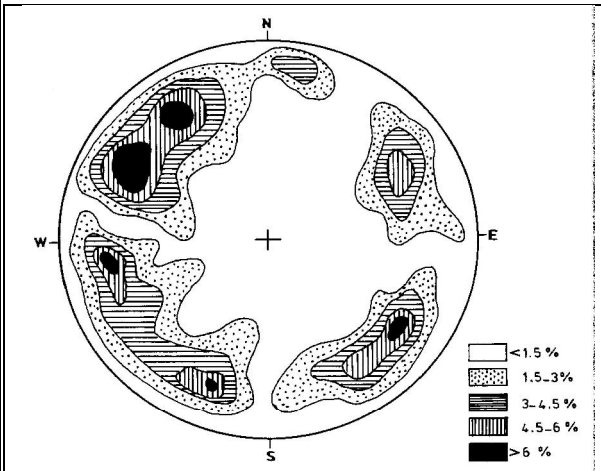


**Fig. (1b): Contour diagram of poles of joints in younger granites, plotted on lower hemisphere, Gabal Gattar area.**

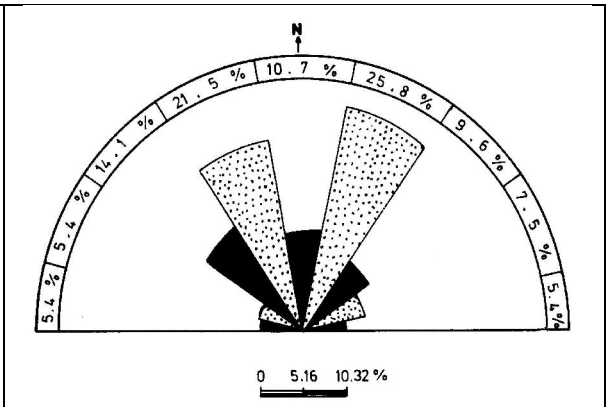


**Fig. (1c): Rose diagram showing the main directional trends of faults at Gabal Gattar area.**

Fig. (2a): Showing a euhedral molybdenite crystal intruded in quartz vein, T.L.200.

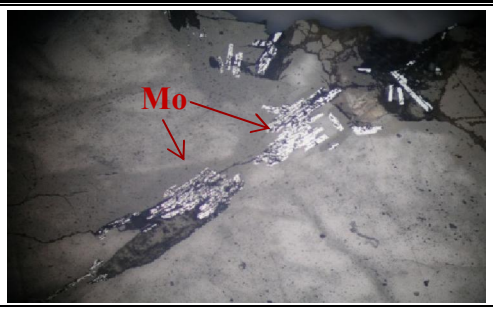


Fig. (2b): Showing needle molybdenite crystal intruded in quartz vein, R.L.200.

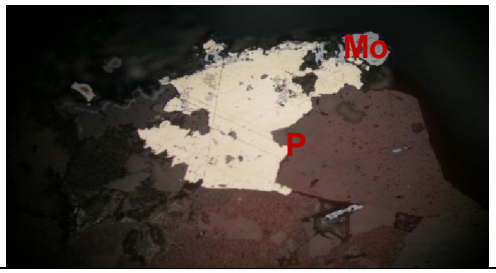


Fig. (2c): Showing molybdenite associated with pyrite crystal. T.L.200.

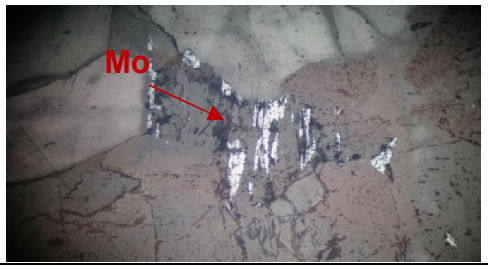


Fig. (2d):Showing needle molybdenite crystal filling fractures in the gangue minerals, R.L.200.

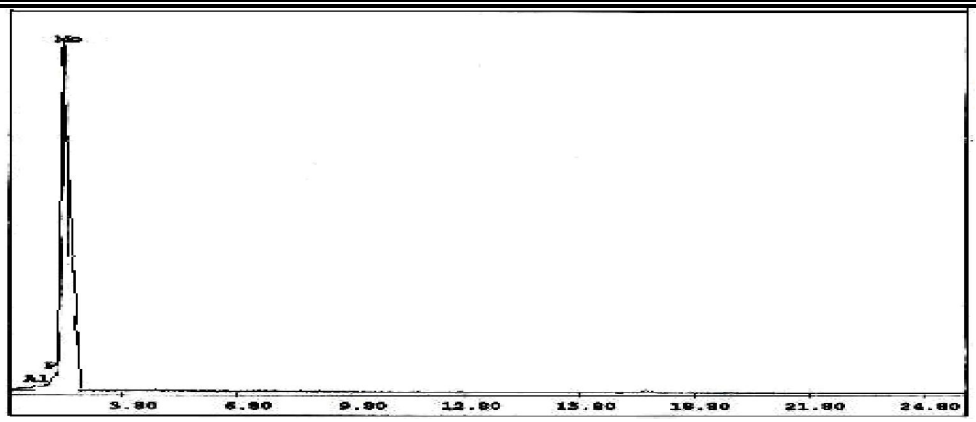


Fig. (2e): EDAX chart for chemical composition of Molybdenite.

Fig. (3a): Showing ferro-molybdenite crystal stained with iron oxides, T.L.200.

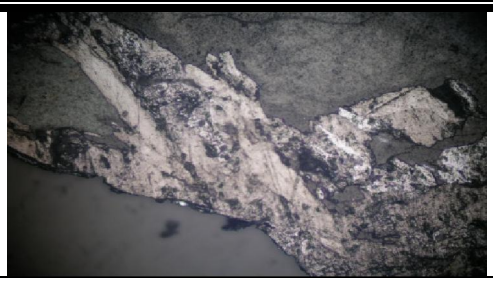

Fig. (3b): Showing ferro-molybdenite crystal developed between quartz crystals, R.L.200.

**Fig. (3c): Showing tabular ferro-molybdenite crystal associated with fine grained hematite and goethite in k - feldspar, R.L.400.**

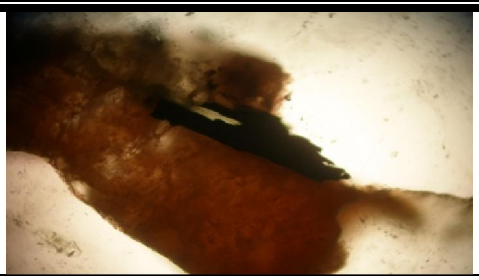

**Fig. (3d): Showing tabular ferro-molybdenite crystal associated with k feldspar, T.L.400.**

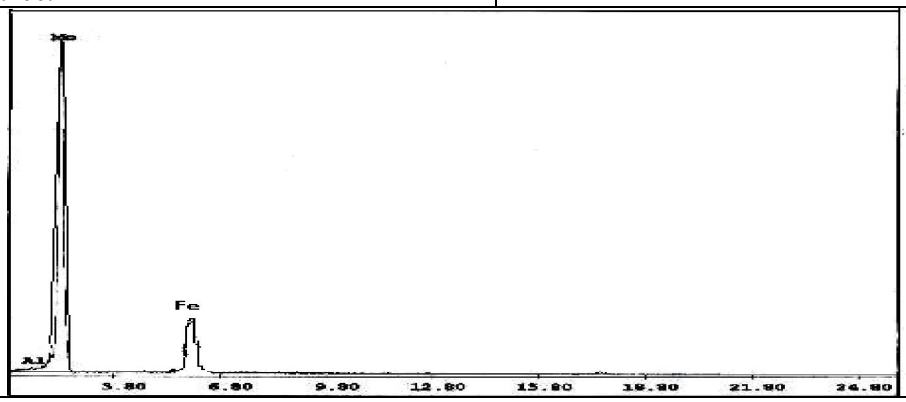


**Fig. (3e): EDAX chart for chemical composition of Ferro-Molybdenite.**

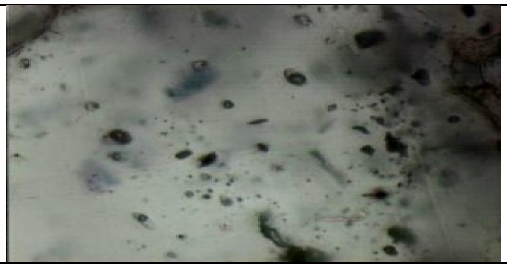

Fig. (4a): Showing the aqueous fluid inclusion in quartz vein. O.L. $X_{150}$

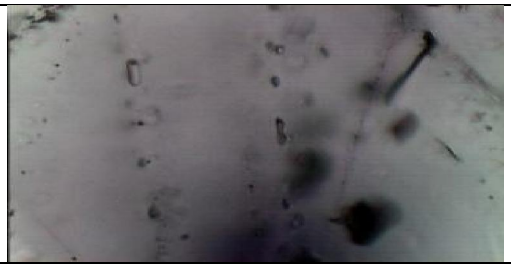

Fig. (4b): Showing the aqueous fluid inclusion in granite. O.L. $X_{150}$

**Discussion**

Homogenization, initial and final ice melting temperatures of 100 fluid inclusions were measured in 12 quartz samples and 80 fluid inclusions were 11 measured in granite samples. The data were processed using Bulk computer program (Baker 2003) to calculate salinities, densities and pressure of the homogenized mineralized fluids. The studied inclusions are of small size and mostly characterize with one aqueous phase. However there is two ranges of eutectic temperature ($T_e$) from –21.2 to -18.9 $^oC$ for granite samples which

coinciding with NaCl water system and from -20.2 to - 45.1 $^oC$ which are much closer to eutectic for chlorite water system containing bivalent ions (notably Ca, Mg) (Franz et al., 2001). Tm ice values in quartz vein samples and granite one represent separate bimodal frequency, the last ice melting temperature ($T_m$) measured the depression were modeled on the system NaCl - $H_2O$ and converted to NaCl equivalent (i.e the amount of NaCl which would produce an equivalent salinity). These temperatures how different population, they range from –21.2 to -10.8$^oC$ for quartz vein samples which strongly indicate high salinity, While ($T_m$) for granite sample range from –8.0 to –1.0 $^oC$ suggesting low salinity of the forming solutions. Total salinities deduced from temperatures ranging from 14.72 to 23.36 eq. wt% NaCl for quartz veins samples and ranging from 1.73 to 11.7 eq. Wt. % NaCl for granitic samples. All investigated inclusions homogenize into liquid state during heating runs, at homogenization temperature ($T_h$) which represent minimum trapping temperature. Most fluid inclusions in quartz vein samples

homogenize at temperature ($T_h$) range from 126.6 to 170.5 $^oC$, while in the granitic samples they homogenize at temperature range from 160.2 to 220.3 $^oC$. Generally fluid inclusions temperature of granitic samples is hotter than quartz vein samples; overall the two parameters ($T_h$) and salinity show correlation in individual quartz veins and granite fluid inclusion samples (Fig.5a). This indicates that the multiple events of cooling can simply be explained by mixing between warm and cool end members of different salinities. The same conclusion can be explained from (Fig.5b).

Mo is then free to migrate and supergene precipitation of Mo in the form of molybdenite, will apply when two conditions are found: (1) where alkaline hydrothermal solution are affected the granites and alternatively, the pH can remain above the stability field of Mo. (2) where there are only minor amounts of pyrite where $H_2S$ fugacity increase. Therefore, when the pH of the aqueous fluid increase ore precipitation occurs (James et al., 1987). The depositional temperatures of molybdenite or rare-elements sulfide from the gas phase increase with increasing $H_2S$ fugacity. This will restrain the ability of S-rich magmatic system to transport volatile Mo at lower temperatures (Bernard et. al., 1990). It can be concluded that the study area there are two stages of mineralization fluids. The oldest recorded fluid is represented by remnants which are only preserved in granite samples as a result of strong acidic hydrothermal fluids where oxidation of molybdenite to ferro-molybdenite in granite is significance for trapping Mo mobility in granite. These fluids are of rich water pure NaCl system, low saline (1.73 to 11.70 wt% NaCl eq.) and with Th values around 200°C. The tectonic history of the region and oxidation patterns confirms the fluid inclusion data that oxidation may have begun at high pressure 19.7 k.bar and reach to about 5.7 k.bar However the pH can remain above the stability field of Mo when alkaline hydrothermal solution are affected the granites and alternatively it will be free to migrate and supergene enrichment of Mo in the form of molybdenite, will apply where there are only minor amounts of pyrite and increasing in $H_2S$ fugacity then precipitate along the week fractured quartz vein surfaces. The detailed fluid inclusions study in the molybdenite bearing-quartz veins is in harmony with the previous modeling where it indicates that the last fluids are homogenized at lower temperature (ranging from 126.7 to 170°C) due to cooling with addition of some divalent salts ($MgCl_2 \pm CaCl_2$) as a result of wall-rock interactions. These fluids are generated under lower pressure (from 4 to 5 k. bar) and characterized by high salinity (14.72 to 23.3 wt% NaCl eq**.).** It can be concluded that subsequent cooling and change in the pH are considered the two factors that have triggered molybdenite precipitation.

**Table (1): Microthermometric results for the studied samples**.

| | | $T_e$°C | $T_m$ °C | $T_h$°C | Pr. (bar) | Salinity (mass% NaCl) |
|---|---|---|---|---|---|---|
| **Fluid Inclusions in** | **Quartz veins** | -43.1 | -15.2 | 144.3 | 4.67 | 18.87 |
| | | -33.6 | -20.3 | 157.6 | 5.3 | 23.11 |
| | | -43.4 | -21.3 | 161.3 | 5.6 | 23.37 |
| | | -20.3 | -12.7 | 143.9 | 4.65 | 16.49 |
| | | -32.1 | -12.3 | 151.7 | 5.00 | 16.44 |
| | | -43.3 | -10.9 | 170.5 | 6.8 | 14.73 |
| | | -32.4 | -14.8 | 134.8 | 4.6 | 18.43 |
| | | -30.3 | -12.4 | 147.4 | 4.9 | 16.66 |
| | | -45.2 | -12.7 | 163.3 | 5.7 | 17.15 |
| | | -20.6 | -16.7 | 138.9 | 4.53 | 20.43 |
| | | -36.6 | -14.3 | 131.7 | 4.83 | 18.46 |
| | | -31.8 | -12.8 | 126.5 | 4.6 | 17.04 |
| | **Granite** | -20 | -8.2 | 200.3 | 12.6 | 11.70 |
| | | -20.2 | -6.1 | 190.7 | 10.3 | 9.21 |
| | | -19.9 | -7.6 | 180.8 | 10.10 | 11.1 |
| | | -18.8 | -5.0 | 220.4 | 19.8 | 7.41 |
| | | -20.2 | -5.3 | 215.8 | 17.7 | 8.10 |
| | | -20.3 | -5.4 | 210.4 | 15.6 | 8.42 |
| | | -21.2 | -5.6 | 200.3 | 12.6 | 8.51 |
| | | -19.8 | -3.7 | 160.4 | 5.64 | 6.00 |
| | | -20.7 | -4.7 | 170.3 | 10.6 | 7.32 |
| | | -21.3 | -2.1 | 215.6 | 17.71 | 3.42 |
| | | -20.3 | -1.0 | 175.7 | 7.40 | 1.74 |

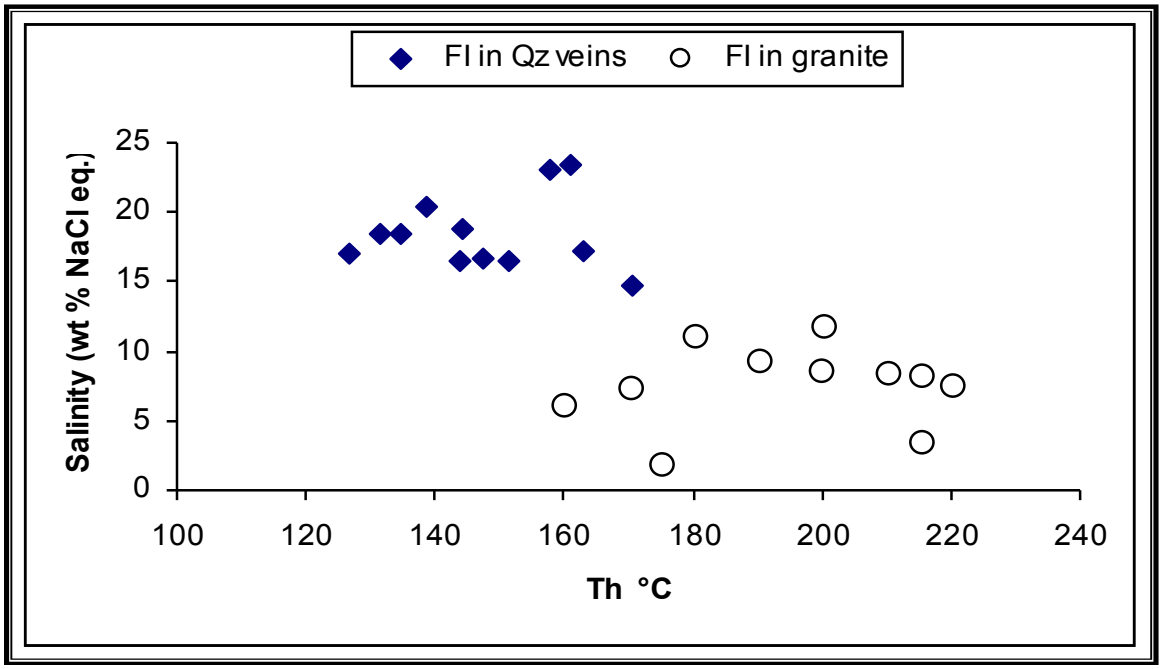


Fig. (5a): Homogenization temperature **( $T_h$°C)**) vs. salinity (wt% NaCl eq.) for selected fluid inclusion samples.

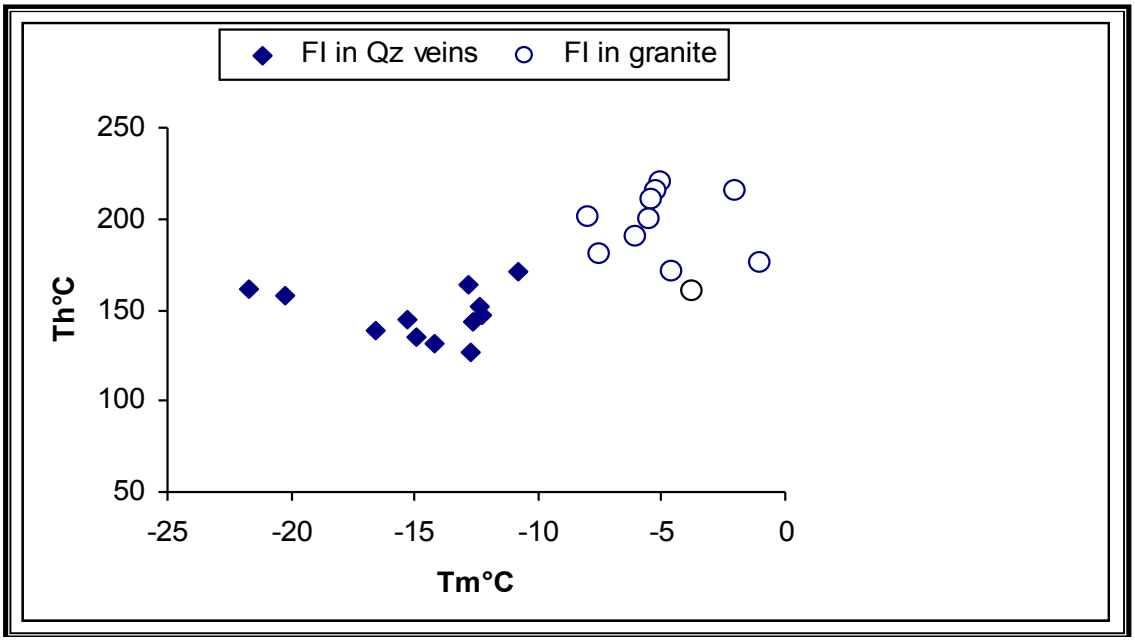


Fig. (5b): Final ice melting temperature **( $T_m$°C)** vs. homogenization temperature **( $T_h$°C)** for selected fluid inclusion samples.

**References**

1. Abd El Hamid, A. A (2006): Geology factors controlling the radon emanation associated with uranium mineralization along wadi Bele, North Eastern Desert, Egypt. M. Sc. Thesis Faculty of Science, Banha Univ., P.189.
2. Amin, N. F (2010): Surface and subsurface structural features controlling Uranium Mineralization at granitic –Hamamat contact, wadi Bele. North Eastern Desert, Egypt. Ph. D. Thesis, Faculty of Science, Ain Shams Univ., P.98.

3. Baker J. Ronald (2003): Fluids, package of computer programs for fluid inclusion studies Program 1: BULK, version 01/03.
4. Bernard A., Symonds R. B. and Rose, W. I. Jr. (1990): Volatile transport and deposition of Mo, W and Re in high temperature magmatic fluids. Applied geochemistry, V.5 Iss.3, p.317-326.
5. Bjorn Qhlander, (1985): Geochemical characteristics of granites associated with Proterozoic molybdenite mineralization in northern Sweden. Chemical geology, V.51 Iss.3-4, p.247-263.
6. Bodnar, R. J., (1993): Revised equation and table for determining the freezing point depression of $H_2O$–NaCl solutions. Geochim. Cosmochim. Acta, V.57, p.683–684.
7. Carten, R. B., Walker, B. M., Geraghty, E. P., and Gunow, A. J., (1988a): Comparison of field-based studies of the Henderson porphyry molybdenum deposit, Colorado, with experimental and theoretical models of porphyry systems: Canadian Institute of mining and metallurgy special, V. 39, p.351-366.
8. Carten, R. B., Geraghty, E. P., Walker, B. M., and Shannon, J. R., (1988b): Cyclic development of igneous features and their relationship to high-temperature hydrothermal features in the Henderson porphyry molybdenum deposit, Colorado: Economic Geology, V. 83, p. 266-269.
9. Dardier A. A. Abu Zeid, K. M. and Gadallia, S. H. (1983): Molybdenite deposits of Gabel Gattar area. Ann Geol. Surv. Egypt XIII: 23-37.
10. El Kaliouby, B. A, El Sayed, M. H and Dawood, Y. H., (2003): Geochemistry and uranium mineralization of the younger granite – Hammamat sediments contact of Egypt. M. E. R. C. Ain Shams Univ., Earth Sci. Ser., V.17, p. 1-23.
11. El Zalaky, M. A. (2002): Interplay of plutonism, faulting and mineralization, North Gabal Qattar peripheral zone, North Eastern Desert, Egypt. M. Sc. Thesis, Fac. Sci., Zagazig Uni., Banha, p. 178.
12. Esmail, E. M. (2005): Subsurface geological constraints controlling uranium mineralization at the northern part of Gabal Gattar, north Eastern Desert, Egypt. Ph. D. Thesis, Ain Shams Univ. p. 194.
13. Franz, L., Romer, R. L., Klemd, R., Schmid, R., Oberha¨nsli, R., Wagner, T., Dong, S., (2001): Eclogite–facies quartz veins within metabasites of the Dabie Shan (eastern China): pressure–temperature– time – deformation path, composition of the fluid phase and fluid flow during exhumation of high-pressure rocks. Contrib. Mineral. Petrol, V.141, p.322– 346.
14. Ghobrial, M. G and Lotfy, M., (1967): The geology of Gabal Gatar and Gabal Dokhan areas, Eastern Desert. Geol. Surv. Egypt, paper No. p. 1976-1982.
15. Helmy, H., M. (1999): Mineralogy, fluid inclusion and geochemistry of the molybdenum-uranium- fluorite mineralizations, Gebel Gattar area, Eastern Desert, Egypt. Interna. Conf. on geochemistry, Alex., Egypt., p. 172-183.
16. Ixer, R. A. and Odling, N. W. (1985): Mineralogy, geochemistry and mineralization of the Ririwai complex, northern Nigeria. Journal of African earth science, V.3 Iss1-2, p185-222.
17. James LeAnderson, J., Schrader E., L., Sandy Brake Dawn Kaback (1987): Behavior of molybdenum during weathering of the Ceresco Ridge porphyry molybdenite deposit, Climax, Colorado and a comparison with the Hollister deposit, North Carolina. Applied geochemistry, V.2 Iss.4-1987, p.399-415.
18. Mahdy, A. I. (1998): Petrological and geochemical studies on the younger granites and Hammamat sediments at Gattar-5. Uranium occurrence, Wadi Balih, North Eastern Desert, Egypt. Ph. D. thesis, Ain Shams Univ., Egypt, p.185.
19. Mahdy, N. M. (2011): Mineralization Studies and mineral chemistry of some radioactive mineralization in Gabal Gattar area, Northern Eastern Desert, Egypt. M. Sc. Thesis, Faculty of science, Ain Shams Univ., Egypt, p.169.
20. Mahdy, N. M, El Kaliobi, B. A, Cora, C., Shalaby, M. H. and El Afandy, A. H. (2015):
21. Perogenesis of U and Mo bearing A2 type granite of the Gattar batholith in the Arabian Nubian Shield, Northern Desert, Egypt: Evidence for the favorability of host rocks for the origin of associated ore deposits. Ore Geology Reviews 71(2015) p.57-81.
22. Rogers, J. J. W. and Adams, J. S. S. (1969): Uranium. In: Wedepohl, K. H. (ed.) Handbook of geochemistry, New York, Springer - Verlag, V. 4, p. 92 B1 to 92 C10.
23. Said R., (1990): The Geology of Egypt. Balkema, Rotterdam, p.731.
24. Salman A. B., Afifi S. Y., Ismail M. and Ammar F. (1999): Uranium potentiality of the South – Gabal Um Tawat Intra Mountain basin, north Eastern Desert, Egypt. First Seminar on Nuclear Row Materials and their technology, p.118-160.
25. Salem H. M, El Foully A. A., El Khoully D. M. (2003): Geological and fluid inclusion constraints on the genesis of hydrothermal

Uranium deposites, Northern Eastern Desert, Egypt. Egyp. Min., p. 163-176.
26. Salman, A. B., El Kholy, D. M. and El Zalaky, M. A. (2005): Relation between granite plutonism, faulting and uranium mineralization in the northern part of Gabal Qattar area, Northern Eastern Desert, Egypt. Al Azhar Bull. Sci., V.16, No.1, p. 23-35.
27. Schürmann, H. M. (1966): The Precambrian along the Gulf of Suez and the Red Sea. Leiden E. J. Brill. p. 404.
28. Seedorff E. and Einaudi M. T. (2006): Henderson porphyry molybdenum system, Colorado: II. Decoupling of introduction and deposition of metals during geochemical evolution of hydrothermal fluids. Economic geology, V.96, p.39-72.
29. Shalaby, M. H. and Moharem, A. F. (2001): Geochemistry and radioelements distribution in the fresh and altered Hammamat sedimentary rocks along Wadi Balih, southern Gabal Um Tawat, north Eastern Desert, Egypt. Sed. of Egypt, V. 9, p. 123-134.
30. Shalaby, M. H, Ammar, F. A, Darwish, M. E and El Sawey, E. H. (2009): Mineralogy and radiometry of the episyenitizaed granitic rocks of Gabal Qattar area, North Eastern Desert, Egypt. Sci. J. Fac. Sci, Minufia Univ. Vol. XXIII, p. 161-188.

2/25/2018